JOURNAL OF MATERIALS SCIENCE **35** (2000) 497–502

Microstructure and properties of zirconia-alumina nanolaminate sol-gel coatings

X. MIAO, B. BEN-NISSAN
Department of Chemistry, Materials and Forensic Science, University of Technology, Sydney, P.O. Box 123, Broadway, NSW 2007, Australia
E-mail: besim.ben-nissan@uts.edu.au

Zirconia-alumina multilayer nanolaminate coatings were applied on stainless steel 316 substrates by a sol-gel dipping method. The coatings were characterised using X-ray diffraction, optical and scanning electron microscopy. The hardness and elastic modulus, the wear resistance and the oxidation resistance of the coatings were measured and assessed. It was observed that the coatings possessed fine grains, fine pores and high retention of tetragonal zirconia phase. The coatings exhibited high hardness and elastic modulus as well as good resistance to oxidation at high temperatures. However, these properties may be influenced by the interactions at the coating/substrate interface.

1. Introduction

There has been an increasing interest in the development of ceramic coatings on metals to improve the resistance to corrosion at high temperatures. Stainless steels are more readily available and less expensive than other high temperature alloys such as nickel- and titanium-based alloys. Thus, stainless steels have been chosen as substrates for corrosion resistant coatings. Ceramic coatings such as zirconia [1–5], alumina [6–8] and silica [9–11] have been applied on stainless steels to improve the oxidation resistance at high temperatures.

Ceramic coatings are conventionally applied on substrates using PVD (e.g., plasma and thermal spraying) [12–14] and CVD [6–9] methods, involving high temperature or high vacuum conditions. Thus, these coating methods are usually expensive and time-consuming. Over the last decade, there has been an increasing interest in technically straightforward and economically inexpensive ceramic coating techniques, such as sol-gel coating [1–5, 11, 15], electrophoretic deposition [11] and electrochemical deposition [8, 16]. In specific applications, the sol-gel coating process has excellent commercial potential, with several advantages over traditional vacuum techniques, including the ability to coat homogeneous films at low temperatures to relatively large and complex substrates continuously.

Sol-gel zirconia coatings on stainless steels [1–5] have attracted much attention. This is mainly because the thermal expansion coefficients of zirconia are relatively close to those of many steels. When zirconia is partially stabilised, it provides the possibility of transformation toughening. Paterson and Ben-Nissan [5] obtained multilayer sol-gel zirconia coatings without cracking and delamination using a special firing schedule. However, high content of monoclinic phase was still present in the coatings. Anast *et al*. [17] reported that cubic or metastable tetragonal zirconia phases in the coatings exhibited higher hardness than monoclinic zirconia phase. With the purpose of developing transformation-toughened ceramic coatings, Aita *et al*. [14] prepared zirconia-alumina nanolaminate coatings on silicon substrates by reactive sputtering deposition. The aim of this paper is to study the feasibility of developing the zirconia-alumina multilayer nanolaminate coatings on stainless steel using the sol-gel technology. Nanolaminates due to their layered structure would have additional toughening effect and the possibility of obtaining comprehensive properties. The current investigation utilises optical, scanning electron microscopy, x-ray diffraction and ultramicro indentation to examine the morphology and mechanical properties of sol-gel zirconia-alumina multilayer nanolaminate coatings.

2. Experimental

Stainless steel 316 grade was used as the substrate material. It was chosen in consideration of the heat treatment required for the coatings. Substrates were polished to 0.3 μm and ultrasonically cleaned in acetone to degrease and ensure the removal of polishing debris. The zirconia precursor solution (~100 ml) used consisted of 21.2 ml zirconium *n*-propoxide (in 63 ml *n*-propanol) as the zirconia source, 5.1 ml acetylacetone to slow down the hydrolysis of the alkoxide, and 8.9 ml polyethylene glycol 200 to slow down the solvent evaporation. The alumina precursor solution (~100 ml) contained 95.4 ml iso-propanol, 5.11 g aluminium isopropoxide, 2.6 ml acetylacetone, 1.35 ml nitric acid. Dip coating was performed in a dry nitrogen atmosphere. The substrates were coated by dipping into and withdrawing from the solutions at a constant speed of about 1 mm/s. The coated substrates were allowed to dry for 15 min

TABLE I Designations of the coated samples

Designation of multilayer coatings	Number of alumina (A) layers	Number of zirconia (Z) layers	Layer sequence
6Z	0	6	/Z/Z/Z/Z/Z/Z
3ZA	3	3	/Z/A/Z/A/Z/A
3ZA-Z	3	4	/Z/A/Z/A/Z/A/Z

in the dry nitrogen atmosphere and hydrolysed in air for 1 h. The coatings were then heat treated by firing to $380 \pm 20\,^{\circ}$C for 0.5 h using the heating rate of 250 °C/h, followed by a second stage firing at $850 \pm 10\,^{\circ}$C for 0.5 h using the previous heating rate and then furnace cooling. To deposit relatively thick coatings it was necessary to build up multiple layers with each layer fired separately to avoid cracking and delamination. Samples coded with 6Z, 3ZA and 3ZA-Z were prepared in this study (Table I). The sample 6Z stands for the stainless steel substrate coated with 6 layers of pure zirconia coating. The sample 3ZA represents the stainless steel coated with 3 sets of alternating zirconia-alumina coatings. The sample 3ZA-Z represents the stainless steel substrate coated with 3 sets of alternating zirconia-alumina coatings plus a zirconia top layer.

The X-ray diffraction was conducted with a Siemens D5000 X-ray diffractometer in glancing angle geometry. The coating morphology and the composition were observed and analysed with the scanning electron microscope JSM 6300 F (JEOL) fitted with an EDS analysis system (eXL LINK). The sol-gel coatings of this study were not coated with any conductive coating to observe the true morphology of the sol-gel coatings. Ultra micro indentation testing was performed using UMIS-2000 system (CSIRO, Division of Applied Physics, Australia). Indentations were made using a triangular diamond pyramid intender and a load of 5 mN. Ultramicro indentation is used for measuring the hardness and elastic modulus of the films [18]. The hardness is indicative of the wear resistance of the multilayer thin films whereas the elastic modulus is indicative of the protective nature of the films because of its strong dependence on any porosity or cracks present [19]. A scratch test was also carried out with the UMIS 2000 system which was adapted for this purpose. Loads of 100 to 600 mN were applied to a spherical diamond indenter of 50 μm radius which traversed at a speed of 1 mm/s. The oxidation resistance of the substrates and the sol-gel coatings was assessed by means of scanning electron microscopy.

3. Results and discussion

3.1. XRD

Fig. 1 shows the XRD patterns of sample 6Z and sample 3ZA-Z. The coatings were approximately 0.6 μm thick, each layer about 100 nm thick. These thin films were transparent to the X-ray, resulting in X-ray diffraction also from the substrates. Two peaks positioned at 2Θ value of 43.76° in Fig. 1a and b belong to the stainless steel. There are also two small peaks with 2Θ value of 33.4° and 35.6°, which correspond to $(Fe_{0.6}Cr_{0.4})_2O_3$ (JCPDS 34-412) and $FeCr_2O_4$ (or $FeO \cdot Cr_2O_3$) (JCPDS 24-511), respectively [2, 4]. These oxides may have resulted from the interfacial reaction between the ceramic coating and the stainless steel substrate. Some oxidation of the substrates was also possible.

There were both monoclinic and tetragonal zirconia phases in the two samples. Comparison of the heights of the m-ZrO_2 (111), t-ZrO_2 (111) and m-ZrO_2 (111) peaks showed that there was larger amount of tetragonal zirconia phase in sample 3ZA-Z (Fig. 1). The tetragonal

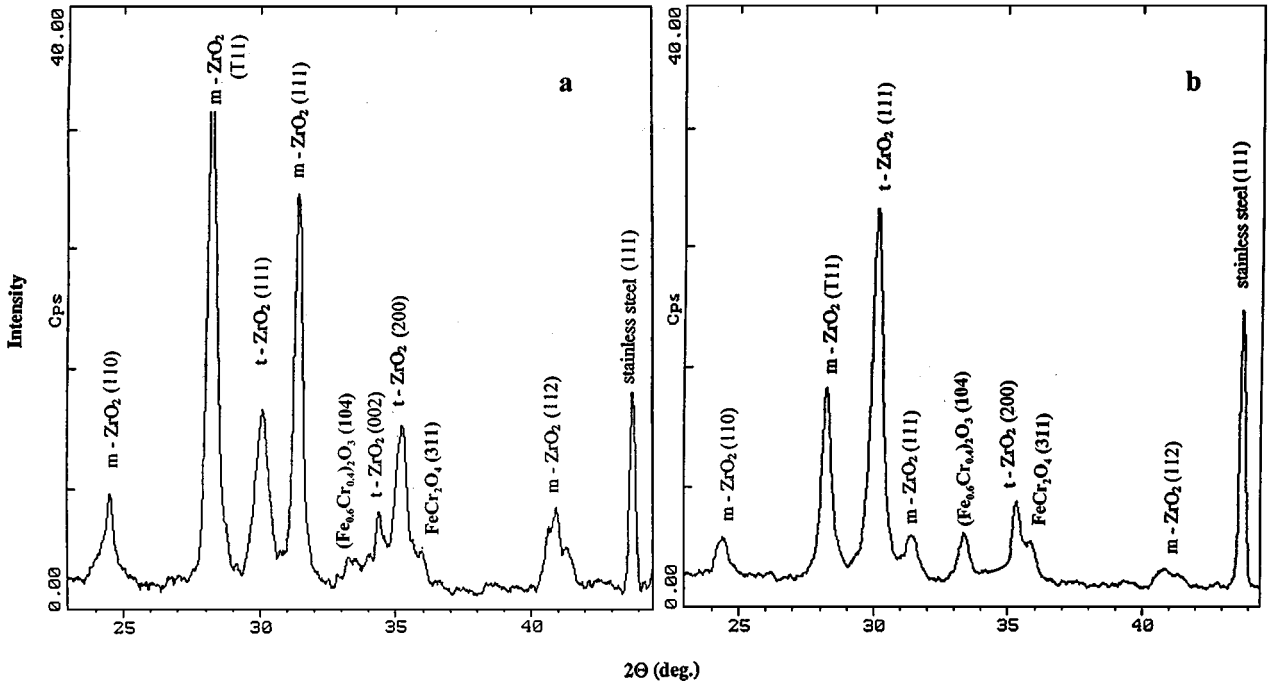

Figure 1 XRD patterns of the coatings of (a) 6Z and (b) 3ZA-Z.

zirconia content of samples 3ZA-Z and 6Z was calculated to be ∼63 wt % and ∼16 wt % respectively using the Garvie and Nicholson's technique [20], i.e., t-ZrO2 wt % = $I(111)_t/(I(\bar{1}11)_m + I(111)_m + I(111)_t)$. This suggests that the addition of alumina layers possibly had the effect of stabilising the tetragonal ZrO_2 phase. The stabilisation of t-ZrO_2 in the presence of Al_2O_3 was also found in the sol-gel derived zirconia mixed with 5–40 wt % alumina [21]. Thus, a nanolaminate with a high wt % of tetragonal zirconia (t-ZrO_2) was produced.

Although sample 3ZA-Z was coated with alumina layers, there was no crystalline alumina phase detected by XRD. However, subsequent energy dispersive spectral analysis confirmed the existence of aluminum. Thus the alumina was possibly in an amorphous state or of such a fine grain size that no definite X-ray diffraction peak could be observed. The alumina could also exist in alumina-zirconia solid solution. It was reported that alumina remained amorphous to 850 °C when mixed with less than 15 wt % ZrO_2 by a sol-gel method [22].

The small amount of iron and chromium mixed oxides detected between the substrates and the sol-gel coatings might also affect the transformation of zirconia. Work on chromium oxide-zirconia catalysts by Sohn *et al*. [23] showed that the presence of chromium oxide was able to stabilise the t-ZrO_2 phase.

3.2. Microscopy

SEM analysis at high magnifications showed that the surfaces of the top zirconia layer of sample 3ZA-Z and the top alumina layer of sample 3ZA were featured with nano-sized grains (or grainy areas) and very fine pores (Fig. 2). Since the coatings were multilayered with each layer fired separately, the most inner layers of the coatings were fired six times for the six-layered coatings, whereas the top layers were fired only once. Therefore, the inner layers are expected to have fewer pores. Even there were pores in the previous fired layers, these pores would be filled at least partially by the subsequent layers of coatings due to the infiltration effect of the sol-gel dipping.

The microstructure of the interface between the coating and the substrate can be imaged by referring to similar studies of zirconia coatings on stainless steels using Auger Electron Spectroscopy (AES) [24] and High-Resolution Transmission Electron Microscopy (HRTEM) [4]. It was shown that the coating close to the substrate contained elements of substrate such as Cr, Fe but no Ni. Below this layer substrate elements steadily returned to their bulk level. On the interface there were elements such as Zr, Cr, Fe, Ni, Si. It was believed that the Ni diffused within the stainless steel substrate replacing the vacancies produced by chromium diffusing to the ZrO_2 coating. From the distribution of elements across the interface analysed by EDS, it was believed that the iron and chromium mixed oxides were formed near or on the interface. According to Shane and Mecartney [2] the iron and chromium mixed oxides led to strong interface bonding.

3.3. Mechanical properties

Fig. 3 shows the load-unload indentation plot for sample 3ZA-Z. Based on the indentation force-penetration depth data, the hardness and the elastic modulus values of the coatings can be calculated [17]. The very low indentation force used resulted in small penetration depth and thus the measured values of hardness and elastic modulus of the coating were not significantly affected by the substrate. The hardness and the elastic modulus measured at 5 mN for the coating were 10.4 ± 0.83 and 240 ± 22 GPa, respectively; for the substrate fired to 850 °C $5.57 \pm$ 0.7 and 130–200 GPa, respectively; and for the as polished stainless steel 3.55 ± 0.6 and 163 ± 16 GPa, respectively. The reasonably high hardness and modulus of the 3ZA-Z coating resulted from the modified microstructure of the coating, namely, high t-/m- zirconia ratio, fine grain size and low porosity. As the films are made up of a number of separately fired layers, it appears that the property changes observed might also be related to the number of layers and of thermal cycles experienced by the sample.

For these alumina-zirconia coatings reasonable wear resistance would be ideal. For wear and corrosion resistance analysis a scratch test was utilized. In the scratch testing the applied loads on the coatings varied from 100 to 600 mN with resultant applied pressures changing from 3 to 12 GPa. Fig. 4 shows the observed wear

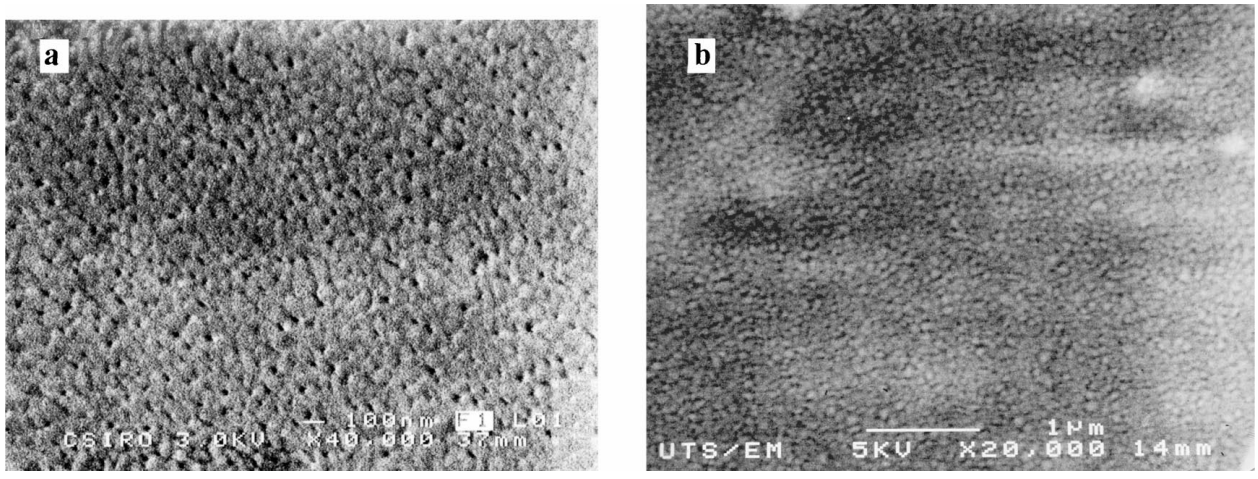

Figure 2 SEM micrographs showing the surface morphology of 3ZA-Z (a) and 3ZA (b) coatings.

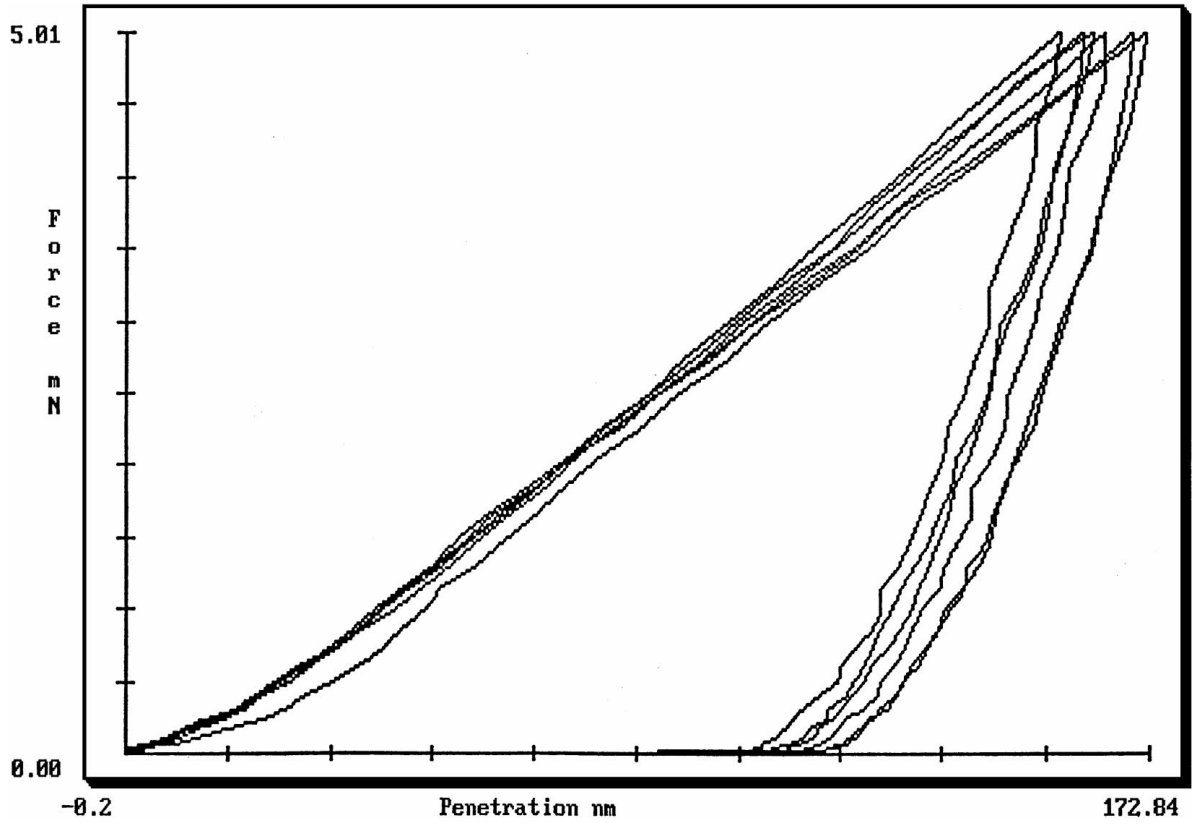

Figure 3 Randomly selected six curves of indentation force versus penetration depth of the 3ZA-Z coating.

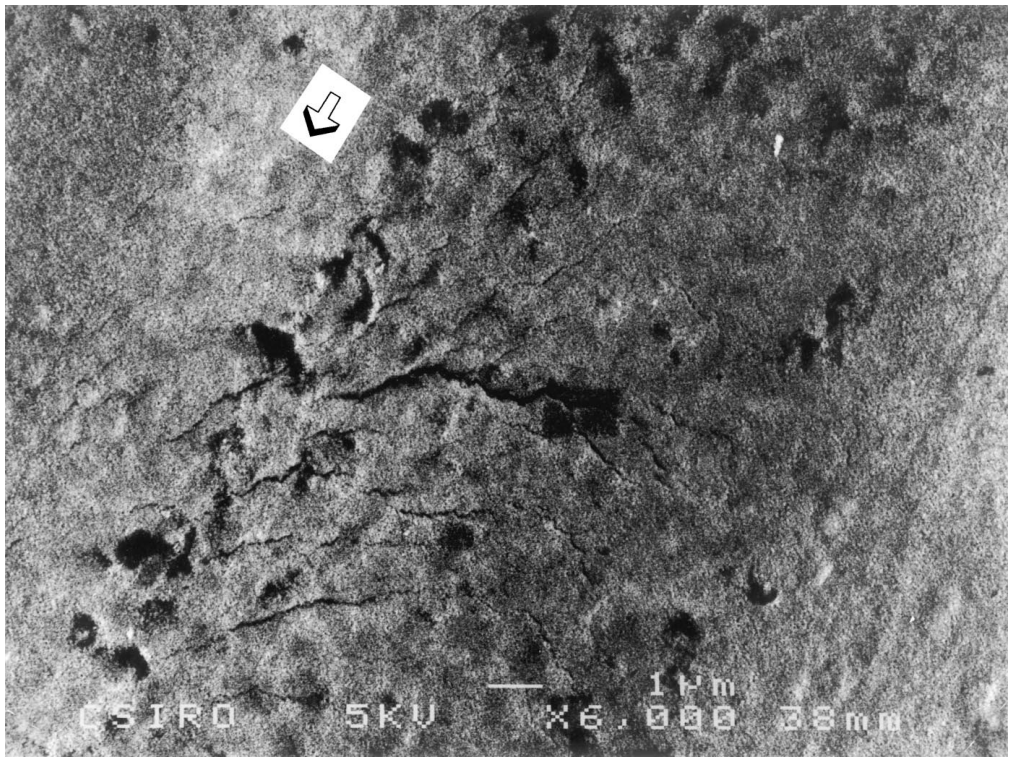

Figure 4 SEM micrograph of the worn 3ZA-Z coating surface scratch tested at 400 mN. The inserted arrow shows the direction of indenter motion.

behaviour of the coating. Some transverse cracks were formed on the wear track at load of 400 mN. At higher load, more transverse cracks were observed, but no delamination had occurred up to 600 mN. This indicated the structural integrity of the coating. The transverse cracking may be explained by the biaxial loading model [25]; a tensile stress on the coating resulted from the friction between the sliding indenter and the coating surface.

3.4. Oxidation resistance

Fig. 5 shows the microstructure of the uncoated stainless steel surface heated to 850 °C for half an hour. The

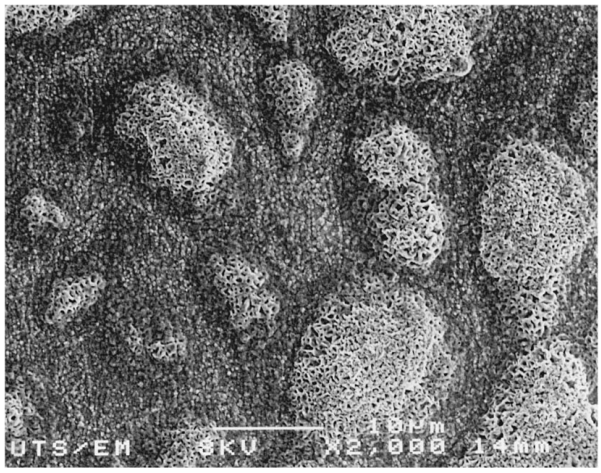

Figure 5 SEM micrograph of the uncoated substrate surface fired at 850 °C for 0.5 h in air.

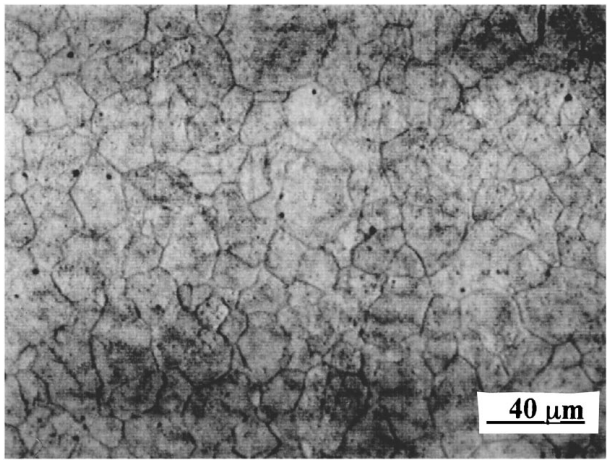

Figure 6 Optical micrograph of the transparent 3ZA-Z coating on the substrate repeatedly heated to 850 °C holding for 0.5 h in air and cooled to 25 °C for six times.

surface was covered with an oxide film. The isolated areas were porous, which resulted in the deterioration of the steel, whereas the continuous areas were fine grain sized with high density. These two different regions of the oxide film have been observed by other workers [4]. Since XRD detected the two phases of $FeCr_2O_4$ and $(Fe_{0.6}Cr_{0.4})_2O_3$ on the oxidised stainless steel and energy dispersive spectral analysis showed that the Fe/Cr intensity ratio was lower in the isolated region than the continuous region, the isolated region could possibly belong to the $FeCr_2O_4$ phase; whereas the continuous region the $(Fe_{0.6}Cr_{0.4})_2O_3$ phase.

Repeatedly fired samples showed that the coated stainless steel surface was intact after subjecting to six cycles of firing at 850 °C for half an hour (Fig. 6). The coating was transparent under optical microscope so that the grain boundaries as a result of firing (thermal etching effect) could be observed clearly. Therefore, the zirconia-alumina nanolaminate coatings could effectively protect the stainless steel against oxidation.

4. Conclusions

Multilayer nanolaminate zirconia-alumina coatings about 0.6 μm thick were successfully applied on stainless steel 316 substrates by a sol-gel dip coating method. The addition of alumina resulted in high retention of tetragonal zirconia phase (~63 wt %). The coatings possessed fine grains, fine pores and high density. Interfacial phases of $FeCr_2O_4$ and $(Fe_{0.6}Cr_{0.4})_2O_3$ were also observed and thought to be responsible for the strong interfacial bonding. The hardness and the modulus of the coatings were 10.4 ± 0.83 and 240 ± 22 GPa, respectively. No delamination of the coatings was observed during the scratch testing at the applied pressure of up to 12 GPa. The nanolaminate zirconia-alumina coatings effectively protect the stainless steel 316 against oxidation at 850 °C.

Acknowledgement

This project was funded by the Australian Research Council Large Grant. The authors would like to thank the following people: M. Anast and R. Wuhrer from the University of Technology, Sydney, for their help with the characterisation; T. Bell and M. V. Swain from the CSIRO Division of Applied Physics for their assistance with the UMIS-2000.

References

1. K. IZUMI, M. MURAKAMI and A. MORITA, *J. Amer. Ceram. Soc.* **72**(8) (1989) 1465–1468.
2. M. SHANE and M. L. MECARTNEY, *J. Mater. Sci.* **25** (1990) 1537–1544.
3. M. ATIK and M. A. AEGERTER, *Journal of Non-Crystalline Solids* **147/148** (1992) 813–819.
4. K. MIYAZAWA, K. SUZUKI and M. Y. WEY, *J. Amer. Ceram. Soc.* **78**(2) (1995) 347–355.
5. M. J. PATERSON and B. BEN-NISSAN, *Surface and Coatings Technology* **86/87** (1996) 153–158.
6. R. W. J. MORSSINKHOF, T. FRANSEN, M. M. D. HEUSINKVELD and P. J. GELLINGS, in "Engineering Ceramics," Vol. 3, edited by G. De, R. A. Terpstra and R. Metselaar (Elsevier Applied Science, London and New York, 1989) pp. 3.484–3.491.
7. M. HALVARSSON and S. VUORINEN, *Materials Science & Engineering A: Structural Materials: Properties, Microstructure and Processing* **209**(1/2) (1996) 337–344.
8. L. ARIES, J. ROY, J. SOTOUL, V. PONTET, P. COSTESEQUE and T. AIGOUY, *J. Appl. Electrochemistry* **26**(6) (1996) 617–622.
9. M. J. BENNETT, *J. Vac. Sci. Techno.* **B2**(4) (1984) 800–805.
10. O. D. SANCTIS, L. GOMEZ and N. PELLEGRI, *J. Non-Cryst. Solids* **121** (1990) 338–343.
11. N. HIDEKI, T. MASAHIRO and M. TSUTOMU, *J. Ceram. Soc. Japan Inter. Ed.* **103**(1) (1995) 78–80.
12. M. T. DUGGER, Y.-W. CHUNG, B. BHUSHAN and W. ROTHSCHILD, *Tribology Transactions* **36**(1) (1993) 84–94.
13. O. UNAL, T. E. MITCHELL and A. H. HEUER, *J. Amer. Ceram. Soc.* **77**(4) (1994) 984–992.
14. M. GAJDARDZISKA-JOSIFOVSKA and C. R. AITA, *J. Appl. Phys.* **79**(3) (1996) 1315–1319.
15. A. BARROW, T. E. PETROFF and M. SAYER, *Surface & Coatings Technology* **76/77**(1–3) pt 1 (1995) 113–118.
16. A. S. M. A. HASEEB, J. P. CELIS and J. R. ROOS, *Materials and Manufacturing Processes* **10**(4) (1995) 707–716.
17. M. ANAST, J. M. BELL, T. J. BELL and B. BEN-NISSAN, *J. Mater. Sci. Let.* **11** (1992) 1483–1485.
18. M. V. SWAIN and J. MENCIK, *Thin Solid Films* **253** (1994) 204.
19. K. F. AMOUZOUVI and L. J. CLEGG, *Scripta Metall. et Mater.* **30** (1994) 1139.
20. R. C. GARVIE and P. S. NICHOLSON, *J. Amer. Ceram. Soc.* **55**(6) (1972) 303–305.

21. K. ISHIDA, K. HIROTA and O. YAMAGUCHI, *ibid.* **77**(5) (1994) 1391–1395.
22. M. BALASUBRAMANIAN, S. K. MALHOTRA and C. V. GOKULARATHNAM, *British Ceramic Transactions*, **95**(6) (1996) 263–266.
23. J. R. SOHN, S. G. RYU, M. Y. PARK and Y. I. PAE, *J. Mater. Sci*. **28** (1993) 4651.
24. M. J. PATERSON, P. J. K. PATERSON and B. BEN-NISSAN, *J. Mater. Res.* **13**(2)(1998) 388–395.
25. B. GUEROULT and K. CHERIF, *J. Canadian Ceram. Soc*. **63**(2) (1994) 132–142.

Received 23 May 1997
and accepted 15 June 1999